MAKARA, TEKNOLOGI, VOL. 15, NO. 2, NOVEMBER 2011: 137-141

IMPROVEMENT OF HIGH TEMPERATURE OXIDATION OF LOW CARBON STEEL EXPOSED TO ETHANOL COMBUSTION PRODUCT AT 700 °C BY HOT-DIP ALUMINIZING COATING

Mohammad Badaruddin

Mechanical Engineering Department, Lampung University, Bandar Lampung 35145, Indonesia

E-mail: rudin_ntust@yahoo.com

Abstract

Low carbon steel (AISI 1005) was coated by hot-dipping into a molten Al-10% Si bath at 700 °C for 18s. After hot-dipping treatment, the coating layers consisted of Al, Si, $FeAl_3$, τ_5-Fe_2Al_8Si, and Fe_2Al_5. The bare steel and the aluminized steel were isothermally oxidized at 700 °C in ethanol combustion product at atmospheric pressure for 49 h. The aluminized steel shows good performance in high temperature oxidation because the formation of Al_2O_3 layer on the coating surface. The growth of iron oxide nodules on the surface coating was accelerated by rapid outward diffusion of Fe-ions due to the presence of H_2O-vapour generated by ethanol combustion. Thus, the oxidation rate of aluminized steel increased, resulting in a substantial mass-gain as the oxidation time increased. After longer exposure, the τ_1-$(Al,Si)_5Fe_3$ phase was completely transformed to the FeAl in the outer layer. The FeAl formed near the steel substrate was due to Fe-atoms diffusing into the Fe_2Al_5 layer when the time and temperature increased.

Keywords: *aluminized steel, ethanol combustion product, low carbon steel*

1. Introduction

The increase in energy demand for the transportation sector has recently led to development of bio-ethanol worldwide to reduce greenhouse gas emissions and consumption of fossil oil. Generally, bio-ethanol as a replacement for methyl tertiary butyl ether (MTBE) is added as a gasoline additive at approximately 11–14% to enhance the octane number and reduce the concentration of harmful substances in the exhaust gas [1]. After combustion of bio-ethanol in an engine, flue gases composed of a rich amount of H_2O and CO_2. The presence of H_2O and CO_2 gases derived from the combustion of diesel fuel-ethanol blend have noticeably been found to increase the reaction rate of the steel in the component of exhaust system of motorcycle and car [2]. Under such conditions, the components of exhaust systems are subject to a great amount of oxidation, resulting in significant mass-loss [3–5]. Therefore, it is important to improve the high temperature resistance of low carbon steel by hot-dip aluminizing coating for decreasing the impact of the alternative fuel on the high temperature corrosion of low carbon steel used as components in exhaust systems.

The present study focuses on an improvement of high temperature oxidation of low carbon steel by hot dip aluminizing coating exposed to ethanol combustion product. After carrying out oxidation tests in this condition, reaction rate, morphology and composition, all are provided to give an insight for better understanding of the oxidation mechanisms.

2. Experiment

Substrates were cut with dimensions of 20 mm × 10 mm × 2 mm from a commercial steel (AISI 1005) with nominal composition (wt.%); 0.06C–0.04S–0.35Mn–0.05P and Fe-balance. The substrate was coated by hot-dipping into the molten Al-10% Si bath at 700 ^oC for 18 s.

The oxidation tests were isothermally performed at 700 °C from 1 to 49 h periods in a horizontal tube furnace with diameter of 100 mm under mixtures of 70% air + 30% C_2H_5OH (ethanol) atmosphere. Dry air was passed at 200 mL/min through a closed isothermal ethanol bath before flowing into the furnace. The temperature of the ethanol bath was maintained at 30 °C. An evaporated ethanol stream table at 30 °C gives the vapor pressure of ethanol of 0.103 atm. The ethanol vapor ignited when blown into the furnace. The specimen was suspended in a crucible boat using a hook made of Grade 304 stainless steel wire and then placed

in the furnace hot zone. The specimen surface was parallel to the direction of gas flow. After a given isothermal oxidation time, the specimens were taken out and cooled in air at room temperature. Each mass-gain data point for the oxidation kinetics was obtained from a different specimen.

After oxidation tests, the phase constituents in the intermetallic layers of all samples were characterized by means of energy-dispersive spectroscopy (EDS) and X-ray diffraction (XRD). The cross-sections and surface morphologies of the specimens were examined using JSM-6390 scanning electron microscopy (SEM) with backscattered/secondary electron image (BEI/SEI) signals operating at 20 kV, and energy dispersive spectroscopy (EDS) using spectrum range of 0–20 keV for a live time of 50 s.

3. Results and Discussion

Oxidation kinetics. The presence of H_2O–CO_2 gases generated by ethanol combustion at 700 °C greatly affect the oxidation kinetics of the bare steel. (Figure 1a). The mass-gain increases gradually with the time and the oxidation kinetics approximately follows parabolic rate law. The aluminized steel exhibited a very low oxidation rate. In order to identify any clear oxidation rates law at 700 °C, the mass-gain is plotted against square root of time (Figure 1b). The kinetics constants of specimens were determined by the linear curve fitting (Figure 1b). The value of the kinetic constants shows at 700 °C for the bare steel, $k_p = 5.31 \times 10^{-9}$ g^2 cm^{-4} s^{-1}, is three orders of magnitude higher than for the aluminized steel: $k_p = 3.20 \times 10^{-12}$ g^2 cm^{-4} s^{-1}. This indicates that the excellent oxidation resistance of the aluminized steel is attributable to formation of continuous Al_2O_3-rich layer [6], as shown in Figure 1a.

There was a substantial mass-gain difference for the aluminized steel exposed to ethanol combustion product at 700 °C. The rate kinetics was found to be initially slow, up to about 9 h. During first 9 h exposure, the oxidation kinetics runs slowly that can be observed as initial incubation periods with the rate constant of 7.72×10^{-13} g^2 cm^{-4} s^{-1}. Change in the slope (Figure 1b) indicates crack formation in the alumina (Al_2O_3) and aluminide layer.

After 9 h exposure, the breakdown of Al_2O_3 layer and the aluminide layer gave way to the development and growth of Fe-rich oxide nodules, considered as the breakaway oxidation (Figure 1b). Figure 2 shows that the local breakdown of the initial protective Al_2O_3 scale led to fast outward diffusion of Fe-ions, resulting from the initial growth of nodules. As the oxidation time was prolonged to 49 h, the kinetics obeyed a parabolic law with a rate constant of 3.20×10^{-12} g^2 cm^{-4} s^{-1}.

As reported by Yoshihara et al. that an additional H_2O in the air atmosphere accelerated more significantly the oxidation of the TiAl alloy by formation of TiO_2 than Al_2O_3, the observed influence of H_2O was attributable to the anisotropic and enhanced growth of TiO_2 [7].

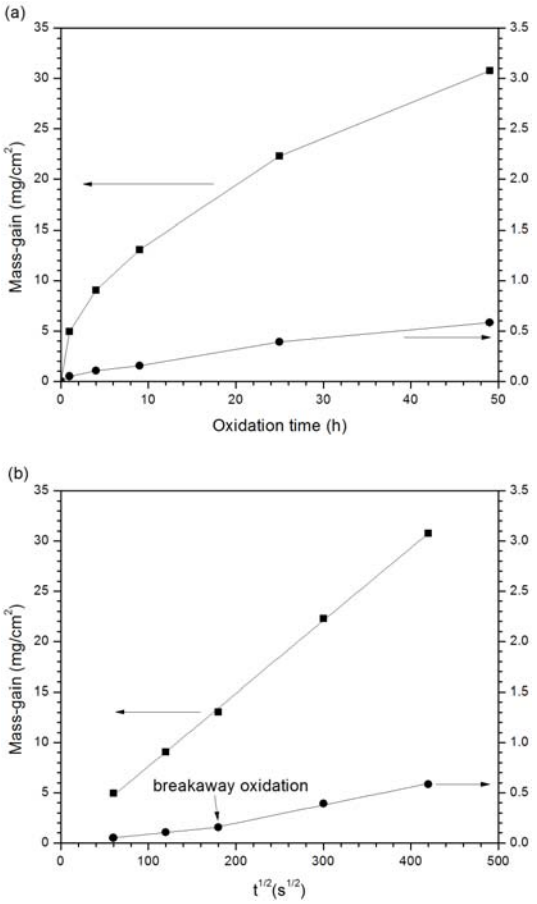

Figure 1. (a) Linear Plot and (b) Parabolic Plot of Oxidation Kinetics, Bare Steel (■), Al–Si Coating (●)

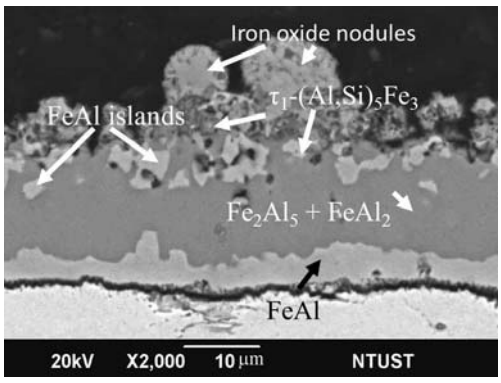

Figure 2. BEI of Cross-Sectional Micrograph Showing the Iron Oxide Nodules Growth on the Aluminized Steel Exposed to Ethanol Combustion Product at 700 °C for 9 h

Moreover, the presence of H_2O and CO_2 generated by simulated combustion gas enhanced the oxidation of Ti–50Al in formation of TiO_2-rich scales but not to Al_2O_3-rich scales [8]. For oxidation of the aluminized steel, the effect of H_2O-vapour in oxidizing gas atmosphere can only be observed by sporadic iron-rich oxide nodules formation as shown in Figure 3.

The large nodule on the aluminide layer grows preferentially along crack direction after 25 h at 700 °C (Figure 3). The rapid iron oxide nodule growth could contribute to the difference in oxidation rates in ethanol combustion product for the aluminized steel. During the very initial stage of oxidation, there is a rapid uptake of oxygen by the coating and the Al_2O_3. Fe-rich oxide nodules are formed on the surface of the coating due to the hydrogen dissolution into the alumina layer [9].

The hydrogen generated by H_2O dissociation provided enhancement in Fe-ions transport through Al_2O_3 scales via aluminum vacancies [9], resulting in a rapid growth of iron oxide nodules. Based on the above description, we can conclude that the influence of water vapor appears mainly through the diffusion of Fe-cations outwardly via Al-rich oxide. Whereas, the effect of CO_2 gas is not yet found giving a contribution with respect to oxidation kinetics of the bare steel and the aluminized steel at 700 °C. Badaruddin [10] has reported that the presence of CO_2 gas in the H_2O-vapour atmosphere is only found at 800 °C in deposition of carbon on the low carbon steel surface.

Microstructural examinations and phase constituents. The surface of morphology of aluminized steel after hot-dipping process shows smooth, and neither crack nor voids are found (Figure 4a). The typical cross-sectional morphology of the as-coated steel is depicted in Figure 4b, where two layers are formed on the steel substrate: topcoat aluminum with Si dissolved and thin layer of Fe-Al-Si intermetallic compound (IMC).

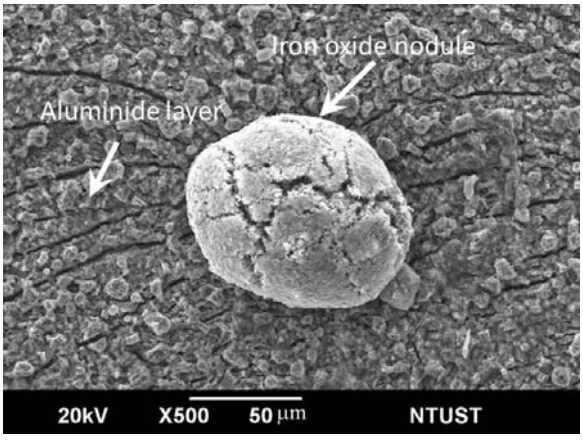

Figure 3. SEM of Surface Morphology of the Aluminized Steel Showing the Iron Oxide Nodule on the Aluminide Surface After 25 h Exposure

The overall thickness of the coating layer is about 25 μm and thin Fe-Al-Si intermetallic layer has of about 4.5 μm in thickness. The XRD patterns of the aluminized samples identified phases formed from the coating surface to the interfacial zone: Al, Si, θ-$FeAl_3$, τ_5-Fe_2Al_8Si, η-Fe_2Al_5, and finally α-Fe (Figure 4c). The

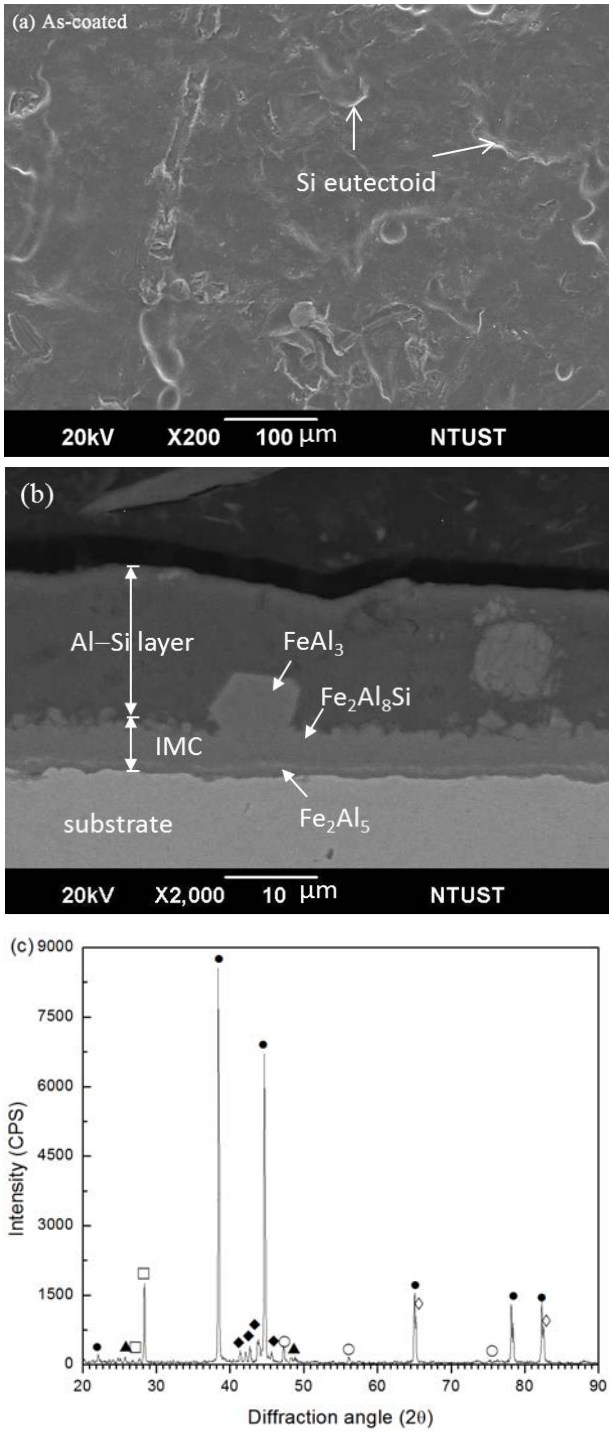

Figure 4. (a) SEM of Surface Morphology, (b) BEI of Cross-sectional Micrograph and (c) XRD Patterns as Coated Specimen, $FeAl_3$ (□), Fe_2Al_8Si (◆) , Fe_2Al_5 (○),Al (●),Si (▲),α-Fe (◊)

intensities of the peaks corresponding to the τ_5 phase and θ-phase can be detected while the peaks related to the η-Fe_2Al_5 phase are small peaks in intensities. However, using grinding technique on the coating layer, it may be observed that small peak intensities of the Fe_2Al_5 phase gradually increased while those of the $FeAl_3$ and the Fe_2Al_8Si phases decreased since the surface of the sample was successively removed by further grinding.

Formation of the intermetallic compounds in Al-rich zone shows that transformation phase is more dominantly controlled by inward diffusion of Al atoms and outward diffusion of Fe atoms to form aluminide layer on the steel substrate.

The cross-sectional micrograph and phases formed in the aluminide layer after oxidation time from 1 to 4 h in ethanol combustion product can be seen in Figure 5. The aluminum coating formed after hot-dip aluminizing process had completely transformed during exposure at 700 °C. For oxidation time of 1 h, the aluminum topcoat disappeared and the aluminide layer formed owing to be the inward diffusion of iron atoms and outward diffusion of aluminum atoms in the coating layer (Figure 5a). It can be seen that the original τ_5-Al_8Fe_2Si and $FeAl_3$ phases were replaced by τ_1-$(Al,Si)_5Fe_3$, and Fe_2Al_5 + $FeAl_2$ layer. Voids also were generated at the interface between the FeAl and the steel substrate due to different diffusion rate between Fe-atom and Al-atom, leading to formation of vacancies, well known as Kirkendall effect [11], as shown in Figure 5a.

As the oxidation time was prolonged to 4 h, the τ_1-$(Al,Si)_5Fe_3$ phase transformed to generate a numerous island of FeAl in outer site of aluminide layer as shown in Figure 5b. The τ_1-$(Al,Si)_5Fe_3$ and the FeAl composition elements are about 51.21Al–37.05Fe–11.74Si and 38.31Al–46.70Fe–14.99Si (at.%), respectively. At the same time, the FeAl kept growing near steel substrate due to Fe-atoms diffused into Fe_2Al_5 + $FeAl_2$ caused Fe_2Al_5 + $FeAl_2$ to be unstable, leading to silicon precipitate into FeAl because the FeAl phase has the higher thermal vacancy while the phase contains of more than 38 at.% Al after rapid cooling time [12-13]. An elemental composition of EDS analysis shows that a large amount of τ_1-$(Al,Si)_5Fe_3$ were formed as precipitation in outer site of the Fe_2Al_5 + $FeAl_2$ layer until the oxidation time was increased to 9 h, as shown in Figure 6.

As the time of oxidation was prolonged to 49 h, a continuous FeAl layer thickened gradually adjacent to the steel substrate since Fe-atoms diffused into the Fe_2Al_5 + $FeAl_2$ layer as time passed due to the dilution of aluminum. The Si solubility in both the FeAl islands and the continuous FeAl layer was similar in atomic composition: 15–17% The thickness of the aluminide layer consisting of a thin Al_2O_3 layer remained constant with the as-coated specimens for all test periods. The presence of those phases was clearly revealed by EDS line scan results (Figure 7).

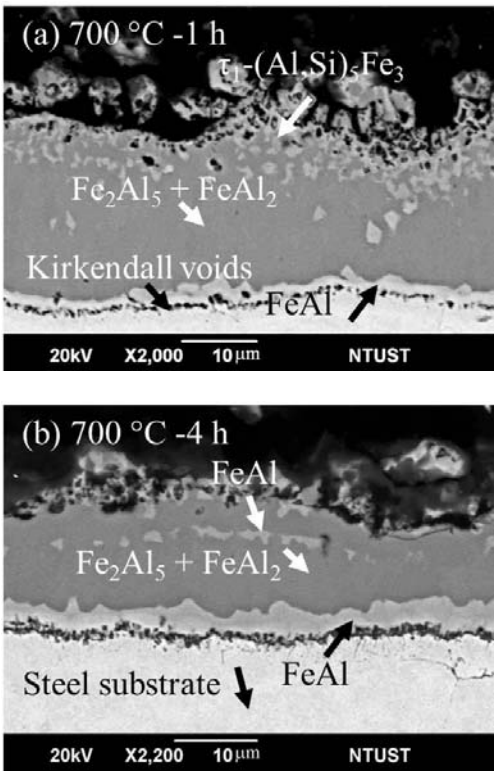

Figure 5. BEI of Cross-Sectional Micrograph of Aluminized Steel Exposed to Ethanol Combustion Product at 700 °C

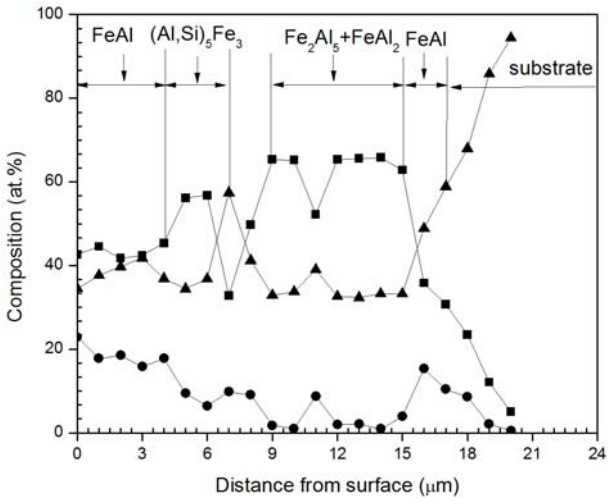

Figure 6. EDS Line Scan Analysis on the Cross-section of Aluminide Layer for the Aluminized Steel Oxidized for 9 h, Al (■),Si (●), Fe (▲)

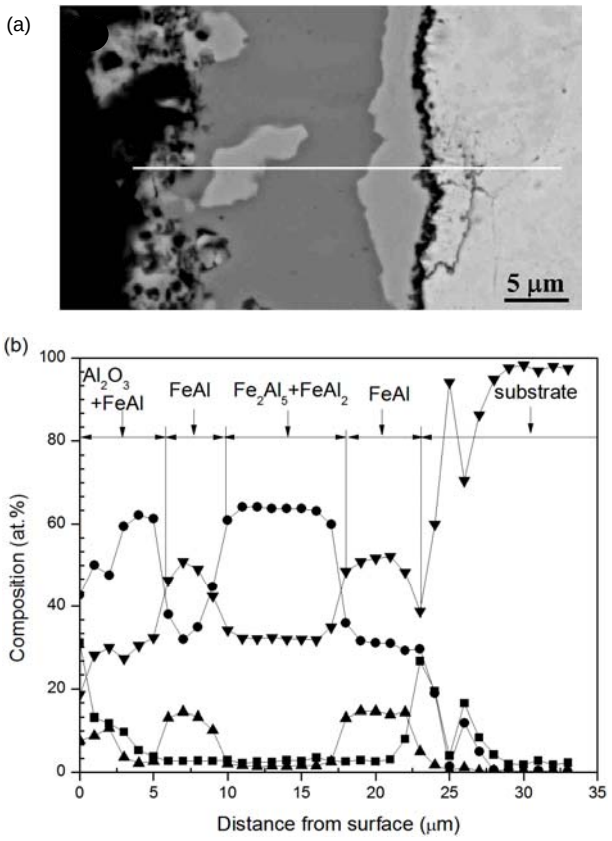

Figure 7. (a) BEI of Cross Sectional Micrograph of the Aluminized Steel and (b) Corresponding to EDS Results of Elemental Composition of O (■), Al (●), Si (▲), and Fe (▼) for the Aluminized Steel After 49 h Exposure

4. Conclusion

The protective Al_2O_3 layer formed on the steel surface greatly improves the high temperature resistance of low carbon steel exposed to ethanol combustion product at 700 °C. The breakaway oxidation was attributed to formation of iron oxide nodules on the aluminde layer, leading to degradation of Al_2O_3 layer on the coating surface due to the presence of H_2O-vapour in the environment. The phases constituents formed in the aluminide layer in ethanol combustion product at 700 °C are consisting of: τ_1-$(Al,Si)_5Fe_3$, Fe_2Al_5, $FeAl_2$ and FeAl. The high–Si content in the FeAl layer on the steel substrate can be barrier Al-atoms to inwardly diffuse in the steel substrate.

References

[1] A. Szklo, R. Schaeffer, F. Delgado, Energy Policy 35 (2007) 5411.
[2] Z. Sahin, O. Durgun, Energy Fuels 23 (2009) 1707.
[3] Y.H. Yoo, I.J. Park, J.G. Kim, H. Kwak, W.S. Ji, Fuel. doi:10.1016/j.fuel.2010.10.058.
[4] R.Y. Chen, W.Y.D. Yuen, Metallur. Mater. Trans A. 40 (2009) 3091.
[5] H.T. Abuluwefa, R.I.L. Guthrie, F. Ajersch, Metallur. Mater. Trans A. 28 (1997) 1633.
[6] L. Sánchez, F.J. Bolívar, M.P. Hierro, F.J. Pérez, Thin Solid Films 517 (2009) 3292.
[7] M. Yoshihara, S. Taniguchi, T. Kubota, J. Japan Inst. Metal. 71 (2007) 16.
[8] S. Taniguchi, N. Hongawara, T. Shibata, J. Japan Inst. Metal. 62 (1998) 542.
[9] C.J. Wang, M. Badaruddin, Surf. Coat. Technol. 25 (2010) 1200.
[10] M. Badaruddin, Ph.D Thesis, College of Engineering, National Taiwan University of Science and Technology (NTUST), Taiwan, 2011.
[11] W.J. Cheng, C.J. Wang, Surf. Coat. Technol. 204 (2009) 824.
[12] Y.A. Chang, L.M. Pike, C.T. Liu, A.R. Bilbrey, D.S. Stone, Intermetallics 1 (1993) 107.
[13] H. Xiao, I. Baker, Scripta. Metall. Mater. 28 (1993) 1411.
[14] W.J. Cheng, C.J. Wang, Mater. Charact. 61 (2010) 467.